

The canopy effect in frequency domain airborne EM

David Beamish

British Geological Survey

Keyworth

Nottingham

NG12 5GG, U.K.

Email: D.Beamish@bgs.ac.uk.

Beamish, D., 2002

The canopy effect in airborne EM. *Geophysics*, 67, 1720-1728.

Corresponding author:

David Beamish

British Geological Survey, Keyworth, Nottingham, NG12 5GG, U.K.

Email: D.Beamish@bgs.ac.uk.

Tel: 0115 936 3432

Fax: 0115 936 3261

Abstract

Airborne electromagnetic (AEM) surveys undertaken at low altitude and small flight separations may be used to provide environmental subsurface assessments. Some of the land quality issues require quite detailed scales (< 1 km) of information. Trial, fixed-wing AEM surveys were conducted in the central English Midlands for such purposes. This paper investigates a specific issue, that of the canopy effect, which needs to be addressed when high-resolution AEM data are to be interpreted accurately. Any elevated feature (typically tree cover) that gives rise to underestimated altimeter readings causes the canopy effect. The inaccurate measurement of sensor height above ground level influences the ground resistivity models that may be obtained from the data.

1D half-space models obtained from conventional, nomogram/look-up procedures together with formal numerical inversion techniques form the basis of the study. Both theory and survey data are used to assess the significance of the canopy thickness, here ranging from zero to 20 m, on the resistivity models obtained. The study uses a small survey area ($1.5 \text{ km} \times 1.5 \text{ km}$) which provides a number of cultural and environmental influences and contains three distinctive canopy zones (forestry, plantation and copse).

The conventional pseudo-layer half-space method has a stated immunity to altitude errors. The method is found to be highly effective in returning resistivity estimates unbiased by altimeter errors. The associated positive apparent depths provide realistic estimates of canopy thickness while, elsewhere, negative values may be returned. Published numerical inversion schemes, used for AEM modeling, do not discuss any corresponding requirement to reduce canopy effect bias. Underestimated altitude measurements introduce false, high resistivity zones with high wavenumber content unless an equivalent pseudo-layer concept is used. The study indicates a requirement for a formal, pseudo-layer (an at-surface perfect resistor of variable depth) to be included in the model when canopy zones are present. The procedure returns stable, zero estimates of canopy thickness in the absence of tree cover and realistic heights of the canopy. In the example considered, resistivity models obtained from a conventional look-up procedure appear more conservative (i.e. of a lower resolution) than their equivalent formal inversion counterparts.

Introduction

AEM surveying can employ frequency-domain or time-domain techniques. The frequency-domain systems, discussed here, currently exist as towed-bird configurations (typically Helicopter HEM systems) and as fixed-wing (wing-tip sensor) configurations. The frequencies employed in the two configurations are similar; the main difference lies in the transmitter-receiver coil separation. HEM bird lengths are typically < 7 m and fixed-wing systems necessarily exceed this by a factor of about 3. A further difference lies in operational height above ground. Typically HEM operates the towed sensor bird about 30 m above ground level while fixed wing systems (with larger dipole moments) may be flown much higher. Early HEM and fixed wing systems used one or two simultaneous operating frequencies and these have been extended both in number and bandwidth. Holladay and Lo (1997) give a review of airborne frequency domain EM.

The fixed-wing AEM system operated by the Geological Survey of Finland (GTK) system was used in a series of trials in the U.K. to acquire detailed data sets in addition to magnetic gradiometer and radiometric information. The data acquired constitute the first high resolution AEM survey information to address specific environmental issues in the U.K. The purpose of the trials was, in part, to assess the case for the inclusion of AEM in future strategic airborne geophysical surveying of the UK. Four areas in the East Midlands were surveyed. Three areas included surveys at low elevation (40 m) using 50-m flight lines. The data discussed in this paper are two selected sub-areas (0.5×0.5 km and 1.5×1.5 km, respectively) from two of the trial survey areas (4.5×1.5 km and 13×9 km, respectively) used in the trials. Particular targets for the EM data included environmentally sensitive zones around conurbations.

The GTK system used in the surveys is described in detail by Poikonen *et al.* (1998). Jokinen & Lanne (1996) describe environmental applications of the system in Finland. The coils are wing-tip mounted (separation of 21.4 m) and are vertical coplanar. Coupling ratios at two frequencies (3.1 and 14.4 kHz) are

recorded simultaneously at 4 Hz. Coupling ratios are here defined as the secondary to primary field ratio multiplied by 10^6 for both the in-phase and quadrature components. The 3.1 kHz data is referred to here as low frequency (LF) and the 14.4 kHz data is referred to as the high frequency (HF) data. Sampling along the flight direction is typically between 10 and 15 m. Elevation information is provided by a Collins radar altimeter. The altimeter has a stated resolution of 10 cm and an accuracy of 0.5 m. Eye-safe laser altimeters can also be used to give sensor elevation above ground. They are also known to suffer from loss of penetration above dense canopy.

The survey data are being assessed for their potential relevance to a number of land-use issues including waste planning and pollution control (Beamish and Kurimo, 2000). Some of these issues require quite detailed, local scale (< 1 km) information. When airborne data are acquired over populated areas, coupling from both at- and near-surface cultural artefacts (e.g. buildings, pipelines, etc.) may occur. The survey data contain examples of the many influences (geological, cultural and environmental) that pose a challenge to valid data interpretation. This study demonstrates that a consideration of canopy cover is also important.

The measured coupling ratios of AEM data are very sensitive to sensor altitude above ground. Although sensor altitude is always recorded, there is no practical way to deconvolve the flight altitude variations from the coupling ratios without recourse to modeling. Resistivity modeling of AEM data was introduced by Fraser (1978) and involves the transformation of single frequency AEM data to a half-space resistivity model. According to Huang and Fraser (2001), the pseudo-layer half-space model, using in-phase (IP) and quadrature (Q) components as input, is the modeling method of choice for displaying apparent resistivity in both plan and section (Sengpiel, 1988; Huang and Fraser, 1996). This is largely because of an immunity of the pseudo-layer model to altimeter errors. Although the usefulness of the pseudo-layer model in relation to canopy cover is often cited, there appear to be no published assessments of its detailed performance.

In addition to the nomogram/look-up table algorithms noted above, formal numerical inversion techniques are now being widely applied to AEM data. The formal techniques can be used to obtain both half-space resistivity estimates (Beamish, 2001) or, in the case of a sufficient number of available frequencies, they can be used to obtain multi-layer resistivity models (Sengpiel and Siemon, 2000). All the formal inversion techniques typically require a minimum input of a single complex response together with the sensor elevation. Once again, the sensor elevation may be in error due to elevated features such as tree canopy.

When assessing the detailed resistivity information obtained at the local scale from the trial data, the issue of tree canopy effects is an important consideration. Across the U.K., forestry is a highly managed activity resulting in many geometrical zones with well-defined boundaries across the landscape. The effects of incorrect altimeter estimates due to tree canopy on resistivity models are considered here. Only 1D, half-space modeling techniques are used. Both the pseudo-layer and formal inversion methods of obtaining resistivity models are investigated. Following a brief description of the relevant theory of AEM resistivity modeling, the sensitivity of coupling ratios to elevation is described. Theoretical effects on resistivity models due to incorrect (underestimated) altimeter estimates are then discussed. A simple survey data example, comprising data obtained over uniform ground with no elevated features, is first used to investigate the observed sensitivity of coupling ratios to flight elevation. This is followed by a detailed assessment of survey data obtained across a 1.5×1.5 km area which contains both a number of cultural and environmental influences and three distinct canopy zones (forestry, plantation and copse). The canopy effect influences the modeling of both recorded frequencies but only the high frequency data are used here to investigate the effect.

AEM resistivity modeling

The most common AEM modeling procedures are those developed and described by Fraser (1978). As discussed by Beard (2000), there are subsets of methods based on the uniform apparent half-space model that involve different combinations of the measured parameters of sensor elevation, IP and Q at each frequency. One of the modeling methods is referred to as the pseudo-layer half-space resistivity. In this method, the sensor altitude above ground level (as measured by a laser or radar altimeter) is not used in the calculation. The pseudo-layer method is used here since it is intended to provide reliable resistivity estimates when the sensor altitude is incorrectly measured due to elevated features. The basis of the method is illustrated in Figure 1.

Using the measured IP and Q coupling ratios at a single frequency, a curve matching (nomogram or look-up) algorithm is used to obtain the apparent resistivity of a half-space (Fraser, 1978; Beard, 2000). As a by-product, the algorithm also returns an estimate of apparent distance (D_a in Figure 1) to the ground surface. Since sensor altitude (h) is also measured, an apparent depth (d_a) may be determined as $d_a = D_a - h$. When $d_a=0$ ($D_a=h$), there are no apparent discrepancies between the model and the data. When $d_a > 0$, it is possible to account for the difference in D_a and h either by the presence of a highly resistive at-surface layer or by an incorrect (underestimated) altitude measurement of h (caused by tree cover or buildings). When $d_a < 0$, Fraser (1978, 1986) suggests that the parameter has no physical meaning other than to indicate that the data and model are inconsistent. Alternatively, when $d_a < 0$, the existence of a conductive layer above a more resistive substratum is often inferred (Sengpiel, 1988; Siemon, 2001).

The success of the method lies in the fact that for a given IP and Q measurement at a specific frequency and coil separation, there exists a unique half-space resistivity and sensor height that fits the measurement. It will be appreciated, however, that there exist a number of ways in which a look-up algorithm can be constructed. Some of the appropriate strategies are considered by Beard (2000) and by Siemon (2001). The algorithm used here is unpublished but is in routine use at the Geological Survey of Finland.

Formal 1D half-space and multi-layer inversion techniques are now being increasingly applied to multi-frequency AEM data sets. The degree to which half-space and multi-layer models are employed is, in practice, a function of the number of survey frequencies and their bandwidth. Paterson and Redford (1986) describe a 2-and 3-layer formal inversion method applied to multi-frequency helicopter EM data. The first layer of the 3-layer model, assumed to be perfectly resistive, was introduced to accommodate geological rather than incorrect altitude issues. Other formal, frequency domain inversion procedures have been described by Beard and Nyquist (1998), Ellis (1998), Fitterman and Deszcz-Pan, M. (1998), Beard (2000) and Sengpiel and Siemon (2000). Sengpiel and Siemon (1998) provide examples of 1D inversion when the resistivity distribution is 3D. None of the formal methodologies appear to require the use of an equivalent pseudo-layer (a high resistance at-surface layer of variable thickness) to provide a corresponding performance to incorrect altitude as that contained in the pseudo-layer IP-Q method.

In this paper, three resistivity modeling procedures are compared. The first is the conventional pseudo-layer IP-Q method (PL-Fraser) developed by Fraser (1978). The method returns apparent resistivity and apparent depth at each measured frequency. No misfit error is provided. The other methods are half-space formal inversions of single frequency data components (again IP and Q). The algorithm uses a typical Marquardt-Levenburg formalism and is described by Beamish (2001). The first inversion uses a single half-space (HS) model while the second inversion incorporates a fixed-resistivity ($100,000 \Omega \text{ m}$), variable thickness layer above a half-space. The second method returns a half-space apparent resistivity and the thickness of the at-surface pseudo-layer together with a misfit error. The second method clearly constitutes a formal equivalent to the existing pseudo-layer concept and is referred to as a pseudo-layer half-space (PL-HS). It will be appreciated that although only 1D half-space models are considered here, the results of canopy altitude errors would equally apply to multi-layer modeling.

Theoretical effects

The sensitivity of the coupling ratios to altitude for the fixed-wing AEM system considered here is shown in Figure 2. The coupling ratios are calculated for a uniform half-space of $20 \Omega \text{ m}$ across a range of altitudes. The 10-m altitude range shown is 'critical' for a nominal survey altitude of 40 m and altitude estimates, which may be underestimated by up to 10 m due to elevated features. Over the 10-m altitude range considered, the response increases with decreasing height by factors of 1.5 (IP) and 1.8 (Q) at low frequency and 1.7 (IP) and 2.2 (Q) at high frequency. For the AEM system considered here, noise figures of $< 5 \text{ ppm}$ (3.1 kHz) and $< 10 \text{ ppm}$ (14.4 kHz) are quoted. These levels of sensor noise imply a theoretical altitude measurement accuracy of less than 4 cm at the low frequency and less than 2 cm at the higher frequency (for a $20 \Omega \text{ m}$ half-space at a survey elevation of 40 m). It can readily be understood that even sub-meter variations in altitude are highly significant.

If we assume that the elevated feature, such as a tree canopy, has no inherent electromagnetic coupling effect with the AEM system, then the measurements are correct with respect to ground resistivity. If the airborne platform could maintain the sensors at a constant height above ground level, then the mapping information in the coupling ratios would be correct across uniform ground and across ground containing elevated features. As can be seen in Figure 2, even 1-m variations in sensor altitude provide significant 'anomalies'. For a departure of 10 m in sensor altitude (flight elevation), the coupling ratios may double when compared with values obtained at the correct (meaning the survey pilot's target) flight elevation of, say, 40 m. The interpretation issues raised by variations in flight elevation can be complex. In practice, the sensitivity of coupling ratios to elevation means that a variety of different amplitude/wavenumber patterns are introduced into every AEM data set by the inherent vagaries of flying an aircraft (the elevation flying pattern).

Using the coupling ratios of the 20 Ω m half-space at an elevation of 40 m (Figure 2) as an example, the PL-Fraser algorithm will always return a half-space resistivity estimate of 20 Ω m. If incorrect estimates of the elevation are used with the 40m elevation response data, the algorithm returns an apparent resistivity of 20 Ω m and apparent depth estimates equal to the difference between the correct elevation (40 m) and the incorrect estimate.

A formal HS algorithm will always return overestimated apparent resistivities if underestimated sensor elevations are used. Figure 3 shows the half-space resistivities returned for the GTK system when a 20 Ω m response obtained at 40 m is used with a set of 9 underestimated elevations from 39 to 30 m. The HS model apparent resistivities for the two frequencies are shown on a logarithmic scale. The high frequency response is most sensitive to elevation errors. When a PL-HS model is used the results follow those obtained with the PL-Fraser method i.e. a constant 20 Ω m half-space is returned and the thickness of the pseudo-layer increases from zero to 10 m.

Uniform ground

To illustrate the sensitivity of coupling ratios to flight elevation, a 0.5 km \times 0.5 km zone within a wider survey area (4.5 \times 1.5 km) has been chosen. The area comprises flat-lying farmland with no elevated structures or tree cover. Only field boundaries (hedges and fences) are contained within the selected area. The geology is a highly uniform, clay-rich Lower Lias sequence that provides pseudo-layer apparent resistivities of between 3.5 to 6.5 Ω m at low frequency and between 3.5 and 11 Ω m at high frequency. The area was flown at a nominal flight elevation of 130 feet (40 m) using 50 m, E-W flight lines. The 0.5 km \times 0.5 km test zone contains 10 flight lines and provides 333 complex measurements at each frequency. The highly conducting nature of the geology provides very large coupling ratios so that altitude sensitivity is highly visible in the data.

The distribution of radar altitude measurements across the test area is shown in Figure 4a. The range extends from 26 to 44 m and peaks (25% of the total) between 36.8 and 38 m. These data imply highly competent survey piloting skills. Despite such skills, flight altitude variations of the order of 10 m are inevitable even over a small-scale sub-sample of the survey area such as this. The variation of high frequency coupling ratios (Q component) with radar altitude across the test area is shown in Figure 4.b. The high frequency ratios exhibit the largest degree of sensitivity to altitude (e.g. Figure 2). Since the area is highly uniform in terms of resistivity and was chosen to contain no elevated structures, the strong inverse correlation between coupling ratio and radar altitude is largely due to survey altitude variations. The equivalent theoretical curves obtained from half-space models of 2.5 and 5 Ω m are shown as the solid and dash lines for comparison. The measurements clearly follow the non-linear behavior predicted by theory. It will be appreciated that the actual subsurface resistivity distribution is not entirely uniform within the limits of the theoretical modeling (uniform half-spaces between 2.5 and 5 Ω m).

In order to demonstrate how flight altitude wavenumber patterns are introduced into coupling ratio mapping information, radar altitude and high frequency (IP component) data are compared for the test area in Figure 5. Figures 5a and 5b display the radar altitude contours in the high (38 to 42 m) and low (28 to 32 m) ranges of the data set. Figure 5b also shows the data sampling of the ten flight lines across the area. Two of the flight lines are labeled A and B for reference. The extremes in flight elevation are, in fact, concentrated on the labeled flight lines. Flight line A was flown predominantly high (38 to 42 m, Figure 5a) and flight line B was flown predominantly low (28-32 m, Figure 5b), in relation to the average flight elevation for this part of the survey (Figure 4a). The high altitude contours are clearly traced by the low interval (6500 to 10500 ppm) high frequency IP-component coupling ratios shown in Figure 5c. Equally, the low altitude contours are clearly traced by the high interval coupling ratios (13000 to 17000 ppm) shown in Figure 5d.

Ground with canopy

Forestry in the U.K. is highly managed resulting in many geometrical zones with well-defined boundaries. Within semi-urban and agricultural areas, small well-established copse zones have been retained throughout the landscape. All these features constitute elevated features and have been found to influence the AEM data sets.

Several test areas have been examined in relation to canopy effects. The example chosen is a 1.5 km × 1.5 km zone taken from a larger survey area (13 × 9 km) in northern Nottinghamshire. The geology comprises the Sherwood Sandstone group. The area was flown at a nominal flight elevation of 130 feet (40 m) using E-W flight lines spaced approximately 50 m apart. The test zone, containing 21 flight lines, is shown in Figure 6. This zone was chosen since it contains only two elevated structures (a farm and a hotel, denoted F and H, respectively) and contains a well-defined, L-shaped conifer plantation, part of the former Sherwood Forest. The test area was chosen to avoid the additional interpretation issues due to conurbations, high-tension power line routes, railways and a regional drainage feature that exist in the vicinity.

The test area contains three former landfills. The former landfill zones are defined here using database records (polygon shape files) which are shown hatched and labeled as L1, L2 and L3 in Figure 6. Landfill L3 extends into the test area as a thin finger polygon in the database records. The landfills constitute environmental targets of the survey. The three landfills ceased operation over 12 years ago and were used for inert and industrial wastes. They have since been covered and landscaped.

Also shown in Figure 6 are selected values of the radar altitude measurements along the flight lines. The altitudes across the test area range from 23 to 54 m. The cross symbols denote all radar altitude measurements < 38 m. Elsewhere along the flight lines, altitude measurements range from 38 to 54 m. Although an exact correlation cannot be expected, there is a degree of correspondence

between low radar altitude recordings and canopy. Probably the most convincing correlation occurs across the two deciduous copse features that occur to the west and north of the single main road (striking NE-SW).

The high frequency (14.4 kHz) data obtained across the test area are used to illustrate the influences of the canopy on the resistivity models that can be obtained from the data. Similar behavior is observed in the low frequency data. Figure 7 shows the apparent resistivity and apparent depth values obtained from the PL-Fraser algorithm. The apparent resistivity results (Figure 7a) range from 35 to 155 Ω m. The anomalous values are selected using gray scale contours for the most conductive interval (30 to 70 Ω m) and single line contours for the most resistive interval (120 to 150 Ω m). Normal 'background' resistivities are judged to lie in the uncounted interval (70 to 120 Ω m). While Landfill 1 (Figure 6) has an associated conductive feature, Landfill 2 has no equivalent expression. The main NE-SW trending road through the area, together with a northward branching track (an unmetalled road), are clearly associated with a semi-continuous conductive feature. The main road (but not the branch track) is the route of a 21-inch cast iron water main pipe.

Apparent depths, contoured in Figure 7b, range from -12 to 19 m. The significant positive values are selected using gray scale contours for the interval from 4 to 19 m. This range of values clearly outlines the main plantation and the two copse features to the north west of the main road. High values of apparent depth, in this case those values > 4 m, are associated with elevated features such as canopy. The actual height of the canopy, although variable, is estimated to be no more than 20 m above ground. Outside the canopy zones, broad areas possess negative apparent depths in the range from 0 to -12 m. If the areas with negative apparent depth are taken to represent a conductive layer over a more resistive substratum, it is not clear what this model represents geologically (i.e. in addition to the landfills, the area contains thin, highly transmissive soils above bedrock).

Results obtained from a half-space (HS) formal inversion that does not include an at-surface pseudo-layer (to account for inaccurate radar altitudes) are presented in Figure 8 as apparent resistivity. The results range from 30 to 380 Ω m. Once again the significant results are selected using gray scale contours for the most conductive interval (30 to 70 Ω m) and single line contours for the most resistive interval (above 120 Ω m). Due to the data range of high resistivity values, a non-uniform contour interval is used and values > 150 Ω m are shown with cross-hatching. Conductive features are now associated with both Landfills 1 and 2 and the feature associated with Landfill 1 extends in a continuous arc, westwards towards the road. The modeling procedure does not produce a significant conductive anomaly pattern along either the main road or along the branch track. The reason for this is an increase in misfit i.e. an inability to precisely model the anomaly that is associated with the road. This is discussed in detail later.

The canopy zone is clearly identified by the high resistivity line contours (> 150 Ω m, cross-hatched). Underestimated radar altitudes clearly cause incorrect high values of resistivity as predicted by theory (Figure 3). The range of the discrepancy (say a maximum canopy height of 20 m in this case) results in a doubling of the apparent resistivity values.

Results obtained from a formal inversion that includes an at-surface resistive pseudo-layer (PL-HS) are now considered. Figure 9 shows the apparent resistivity and apparent thickness of the at-surface resistive layer obtained by this procedure. Polygons associated with the three Landfills are shown as hatched areas in Figure 9a. The apparent resistivity results range from 21 to 153 Ω m. Once again the significant results are selected using gray scale contours for the most conductive interval (30 to 70 Ω m) and single line contours for the most resistive interval (120 to 150 Ω m). In areas where no canopy exists, the apparent resistivity distribution is equivalent to that obtained in the previous analysis (Figure 8) and Landfills 1 and 2 are associated with conductive zones. A conductive feature is seen displaced from Landfill polygon 3. It is possible, and

this has been confirmed in other areas, that the positional information obtained from historical records is not always accurate and the features observed from AEM data sometimes offer a more reliable indicator of location and extent.

This particular model also better fits the anomaly associated with the main road and track (see below) and traces the same conductive, road-associated zone seen in the PL-Fraser results (Figure 7a). The central resistive zones ($>120 \Omega \text{ m}$) seen previously in the PL-Fraser results are also observed in the present results. The two zones straddle canopy and open ground.

The apparent thickness results shown in Figure 9b range from -2 to 20.5 m. The positive values (0 to 20 m) show a high level of correspondence with those of the apparent depth returned by the PL-Fraser algorithm (Figure 7b). The data have been contoured at the same interval of 4 m. The zero and negative level contours are effectively noise and the onset of canopy is clearly observed when apparent thickness is greater than 4 m. Tree canopy does not constitute a uniform surface to airborne altimeters. Variations in woodland density and tree type provide an undulating surface. The apparent thicknesses observed across the canopy areas in Figure 7b are predominantly $< 16 \text{ m}$ and appear representative of the true heights of the woodland.

The modeling discussed here has been limited to assessments of half-space resistivity models. The accuracy of such models depends on the validity of the half-space assumption that can be both survey (altitude and frequency) and site specific. Theoretically, when the half space assumption becomes less valid, errors (or different averages) could be introduced into both the estimates of pseudo-layer thickness and the half-space resistivity model. In the example used, the greatest departures from the half-space assumption would most likely occur in the vicinity of the resistivity gradients associated with the road and landfills. Empirically it is observed (Figure 9b) that in such regions the estimate of pseudo-layer thickness remains uniform and realistic (an apparent accuracy of a few metres).

In contrast to the PL-Fraser algorithm, formal inversion methods provide a measure of misfit between data and model. The misfit can play a critical role in understanding the behavior of models that are often produced by 'automatic' inversion schemes (Beamish, 2001). A detailed example is provided by examining the data and models obtained along one of the E-W survey flight lines. Line 172, indicated in Figure 6, traverses the road and canopy but is displaced from the conductive features. The high frequency IP component results along Line 172 are used for illustration. Figure 10a shows the observed data (symbols) and the IP response of the two formal inversion methods (HS and PL-HS). Figure 10b shows the apparent resistivities obtained by the two formal inversion methods together with those obtained by the PL-Fraser method.

The high amplitude anomaly associated with the road is circled and the E-W extent of canopy cover along the flight line is indicated. The HS model response shows a large misfit over the central four points of the road anomaly. Across the canopy zone, the HS model response again shows a large misfit; in this case it is due to incorrect altitude data. In contrast, the PL-HS model response tracks the observed data with small misfits. To the east of 457 km, a small but persistent bias between observed and modeled data is evident. This is usually due to the breakdown of the half-space assumption i.e. the single frequency data across this zone could only be accurately modeled using a minimum of two layers.

The road anomaly is equally well modeled as a conductive feature, below an at-surface resistive zone, by the PL-Fraser and PL-HS algorithms (Figure 10b). The excursion to high and unrealistic values of resistivity when altitude is underestimated across the canopy zone is very evident (HS model, Figure 10b). High wavenumber estimates, presumably caused by undulating canopy height, are also observed. To the east of the canopy zone the formal inversion results are identical (as expected) however both are significantly lower than their PL-Fraser model counterparts.

Conclusions

This paper has discussed the canopy effect in relation to airborne EM measurements. Both theory and survey data have been used to assess the significance of underestimated altitude on resistivity models obtained from AEM data. The sensitivity of coupling ratios to sensor elevation is such that sub-meter accuracy of height above ground surface is required. Although only the canopy effect has been discussed, the results would equally apply to any elevated structure that does not produce an electromagnetic response.

From the survey altitude data obtained over uniform ground it is clear that, even with highly competent piloting skills, sensor altitudes may vary by 10 m at a nominal survey height of 40 m even over small areas within a wider survey. In the example used, the survey data obtained over canopy indicates that 'typical' deciduous and conifer plantations introduce underestimated altitude measurements in the range from several to just over 20 m.

The performance of three half-space modeling methods has been compared. The pseudo-layer half-space method introduced by Fraser (1978) has a stated immunity to altitude errors. The method was found to be highly effective in returning resistivity estimates 'unbiased' by the altitude errors. The positive apparent depths obtained by the procedure clearly outline the main canopy zones and their magnitudes are realistic.

A comparison of two formal inversion procedures indicates a requirement for a formal pseudo-layer (an at-surface perfect resistor of variable depth) to be included in the model when canopy zones are present. In the absence of a formal pseudo-layer, canopy zones introduce false, resistive zones with an associated high wavenumber content. When the pseudo-layer is included in the inversion procedure, the estimated thickness appears to provide appropriate zero level information together with appropriate heights (= thickness) of the tree cover.

The example test area contains a number of cultural and environmental features that influence the resistivity distribution. Ultimately a full understanding of their

influences can only be achieved using additional ground-truth studies. Despite their broad agreement, there are detailed and significant differences between the half-space resistivity models returned by the two pseudo-layer procedures. As discussed by Beamish (2001), it appears that the PL-Fraser look-up algorithm often provides a reliable but conservative estimate of the resistivity distribution. Thus in the case of the three Landfills within the test area, the look-up algorithm appears to either limit or omit their presence in the resulting resistivity model.

The modeling and interpretation issues discussed here arise due to the imprecise measurement of sensor altitude with respect to ground level. The areal coverage, either on the ground surface or across a canopy, will be different for a laser altimeter, a radar altimeter (used here) and an AEM system. The different lateral scales of information will undoubtedly give rise to different averages in the estimates of height information. Two possible improvements to aid modeling would be for the on-board avionics to record accurate (sub-meter) barometric height (e.g. Sengpiel & Siemon, 2000) or to establish equivalent accuracy in the elevation information provided by differential global positioning systems already used for position information.

Acknowledgments

The author wishes to thank reviewers and the associate editor for constructive advice.

The survey data discussed here were obtained as a collaborative venture between the British and Finnish Geological Surveys (BGS and GTK). The BGS wishes to thank Maija Kurimo and the GTK team for their dedication and professionalism during the survey operations. We are grateful to the Department of the Environment, Transport and the Regions and the Environment Agency for their co-sponsorship of the acquisition of the survey data. This report is published with the permission of the Director, British Geological Survey (NERC).

References

Beamish, D. and Kurimo, M., 2000, Trial airborne EM surveys to assess minewater pollution in the UK, 62nd EAGE Extended Abstracts, Vol. 1, D-22, Glasgow, UK.

Beamish, D., 2001, A study of conventional and formal inversion methods applied to AEM data: J. Appl. Geophys, submitted.

Beard, L.P. and Nyquist, J.E., 1998, Simultaneous inversion of airborne electromagnetic data for resistivity and magnetic permeability: Geophysics, **63**, 1556-1564.

Beard, L.P., 2000, Comparison of methods for estimating earth resistivity from airborne electromagnetic measurements: J. Appl. Geophys., **45**, 239-259.

Ellis, R.G., 1998, Inversion of airborne electromagnetic data: Exploration Geophysics, **29**, 121-127.

Fitterman, D.V. and Deszcz-Pan, M., 1998, Helicopter EM mapping of saltwater intrusion in Everglades National Park: Exploration Geophysics, **29**, 240-243.

Fraser, D.C., 1978, Resistivity mapping with an airborne multicoil electromagnetic system: Geophysics, **43**, 144-172.

Fraser, D.C., 1986. Dighem resistivity techniques in airborne electromagnetic mapping. In: Palacky, G.J. (Ed.), Airborne Resistivity Mapping, Geological Survey of Canada, Paper 86-22, pp. 49-54.

Holladay, S. and Lo, B., 1997, Airborne frequency-domain EM – Review and preview, *in* Gubins, A.G., Ed., Proceedings of Exploration 97: Fourth International Conference on Mineral Exploration, 505-514.

Huang, H. and Fraser, D.C., 1996, The differential parameter method for multifrequency airborne resistivity mapping: *Geophysics*, **55**, 1327-1337.

Huang, H. and Fraser, D.C., 2001, Mapping of resistivity, susceptibility and permittivity of the earth using a helicopter-borne electromagnetic system: *Geophysics*, **66**, 148-157.

Jokinen, T. and Lanne, E., 1996, Airborne geophysics in mapping contaminant plumes from landfills: *SAGEEP Extended Abstracts*, Keystone, Colorado, 981-995.

Paterson, N. and Redford, S.W., 1986, Inversion of airborne electromagnetic data for overburden mapping and groundwater exploration, *in* Palacky, G.J., Ed., *Airborne Resistivity Mapping*, Geological Survey of Canada, Paper 86-22, 39-48.

Poikonen, A., Sulkanen, K., Oksama, M. and Suppala, I., 1998, Novel dual frequency fixed wing airborne EM system of Geological Survey of Finland (GTK): *Exploration Geophysics*, **29**, 46-51.

Sengpiel, K.-P., 1988, Approximate inversion of airborne EM data from a multi-layered ground: *Geophys. Prosp.*, **36**, 446-459.

Sengpiel, K.-P. and Siemon, B., 1998, Examples of 1-D inversion of multifrequency HEM data from 3-D resistivity distribution: *Exploration Geophysics*, **29**, 133-141.

Sengpiel, K.-P. and Siemon, B., 2000, Advanced inversion methods for airborne electromagnetic exploration: *Geophysics*, **65**, 1983-1992.

Siemon, B., 2001, Improved and new resistivity-depth profiles for helicopter electromagnetic data: *J. Appl. Geophys.*, **46**, 65-76.

Figure Captions

Figure 1. Illustration of parameter relationships involved in the pseudo-layer half-space calculation. The sensor separation is r . The on-board altimeter provides a correct elevation of h or underestimated h^* when elevated features are encountered. Apparent distance (to half-space) is D_a and formulae give the apparent depth (d_a) below ground surface.

Figure 2. Variation of coupling ratios with altitude above a 20Ω m half-space (coil separation = 21.36 m). Low frequency (LF=3.1 kHz) and high frequency (HF=14.4 kHz), in-phase (IP) and quadrature (Q) components.

Figure 3. Apparent resistivity results obtained by numerical inversion of a 20Ω m half-space response at 40 m. The recorded elevation is an underestimated elevation due to canopy with height ranging from 0 to 10 m. Low frequency (LF=3.1 kHz) and high frequency (HF=14.4 kHz) results.

Figure 4. Survey results obtained across uniform ground (0.5×0.5 km). (a) Histogram of radar altitudes. (b) Variation of high frequency (HF=14.4 kHz), Q-component coupling ratios with radar altitude. Superimposed curves are theoretical Q-components response estimates for half-spaces of 5 and 2.5Ω m.

Figure 5. Survey results obtained across uniform ground (0.5×0.5 km). (a) Radar altitude in the range 38–42 m, contour interval 1 m. (b) radar altitude in the range 28– 32 m, contour interval 1 m. (c) High frequency, in-phase coupling ratios in the range 6500-10500 ppm, contour interval 500 ppm. (d) High frequency, in-phase coupling ratios in the range 13000-17000 ppm, contour interval 500 ppm.

Figure 6. Map of $1.5 \text{ km} \times 1.5 \text{ km}$ canopy test survey area. Canopy shown as pattern fill with symbols of tree type. F and H denote a farm and a hotel, respectively. Roads are denoted in grey. Cross symbols denote radar altitudes,

along E-W flight lines, < 38 m in elevation. Three closed and covered landfills are shown as cross-hatched polygons, labeled L1, L2 and L3. Flight line (FL) 172 is shown as a horizontal line. The base map is simplified after the 1995 Ordnance Survey 1:50000 Landranger Series map.

Figure 7. Conventional pseudo-layer half-space results obtained using the high frequency (14.4 kHz) data. (a) Apparent resistivity contoured as 30-70 Ω m (gray scale), 70 to 120 Ω m (line contours only). (b) Apparent depth contoured continuously, with gray scale used for values > 4 m. Negative values shown in cross-hatch.

Figure 8. Half-space formal inversion results using the high frequency (14.4 kHz) data. Apparent resistivity contoured as 3-70 Ω m (gray scale), 120-150 Ω m (line only contours), 150-350 Ω m (line contours with cross-hatch).

Figure 9. Formal inversion pseudo-layer half-space result obtained using the high frequency (14.4 kHz) data. (a) Apparent resistivity contoured as 30-70 Ω m (gray scale), 70 to 150 Ω m (line contours only). (b) Thickness of pseudo-layer contoured continuously, with gray scale used for values > 4 m. Negative values shown in cross-hatch.

Figure 10. High frequency (14.4 kHz) observations and models obtained along flight line 172. (a) Observed IP-component (symbols), modeled IP-component response using formal half-space (HS) and pseudo-layer half-space (PL-HS) inversion. (b) Half-space apparent resistivities obtained using conventional pseudo-layer (PL-Fraser) and formal half-space (HS) and pseudo-layer half-space (PL-HS) inversion.

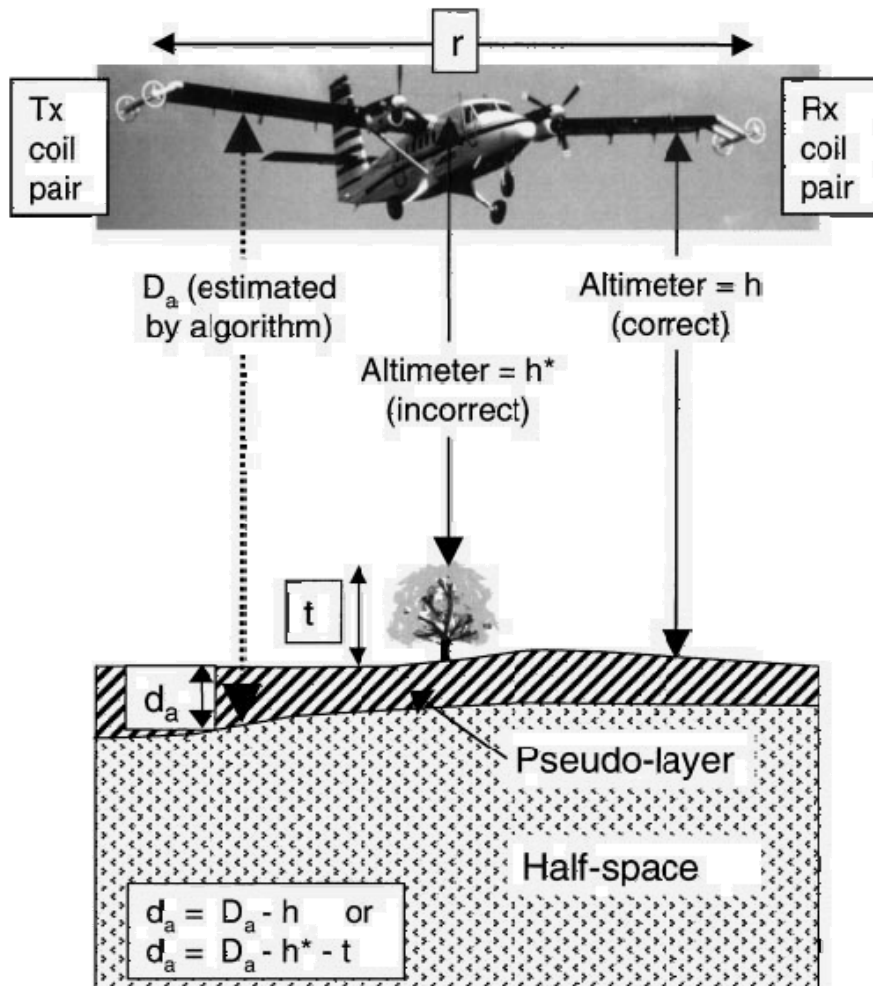


Figure 1. Illustration of parameter relationships involved in the pseudo-layer half-space calculation. The sensor separation is r . The on-board altimeter provides a correct elevation of h or underestimated h^* when elevated features are encountered. Apparent distance (to half-space) is D_a and formulae give the apparent depth (d_a) below ground surface.

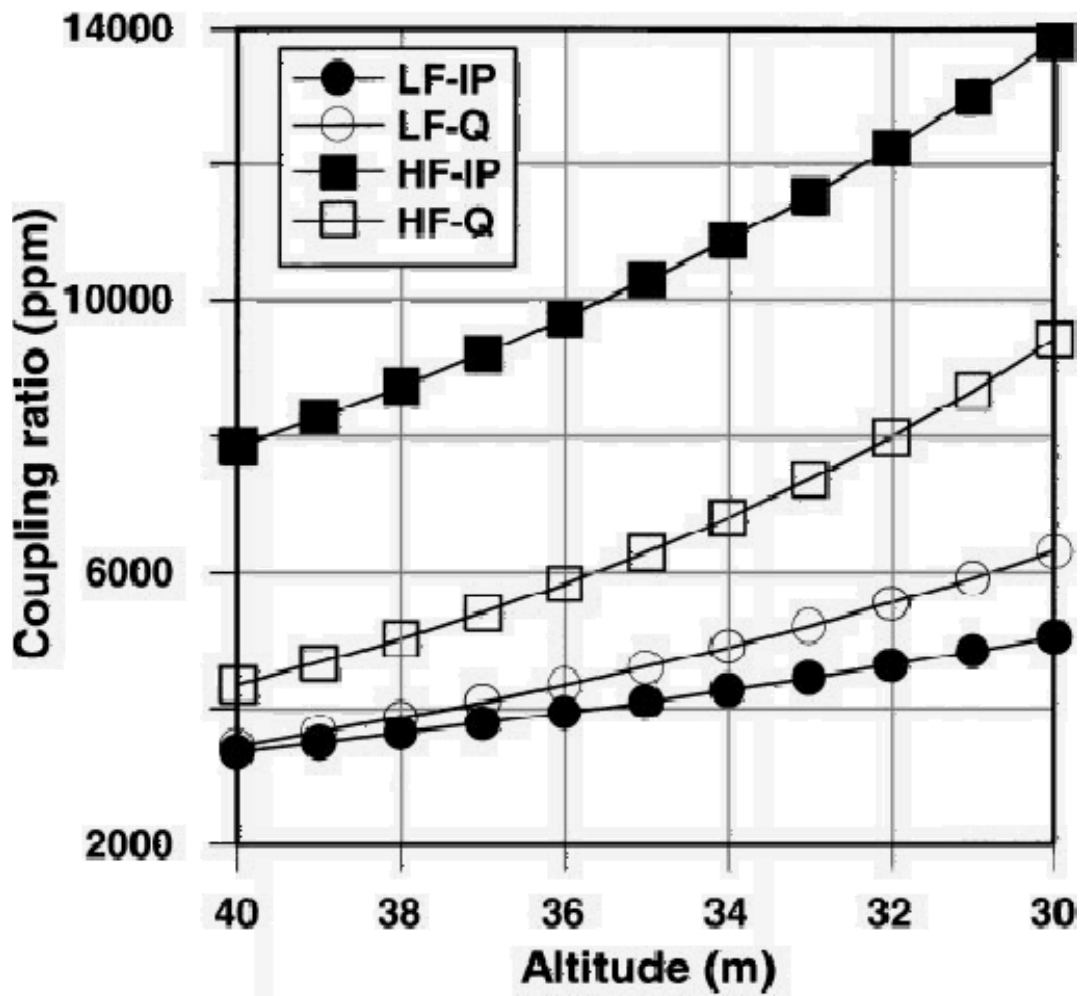


Figure 2. Variation of coupling ratios with altitude above a 20Ω m half-space (coil separation = 21.36 m). Low frequency (LF=3.1 kHz) and high frequency (HF=14.4 kHz), in-phase (IP) and quadrature (Q) components.

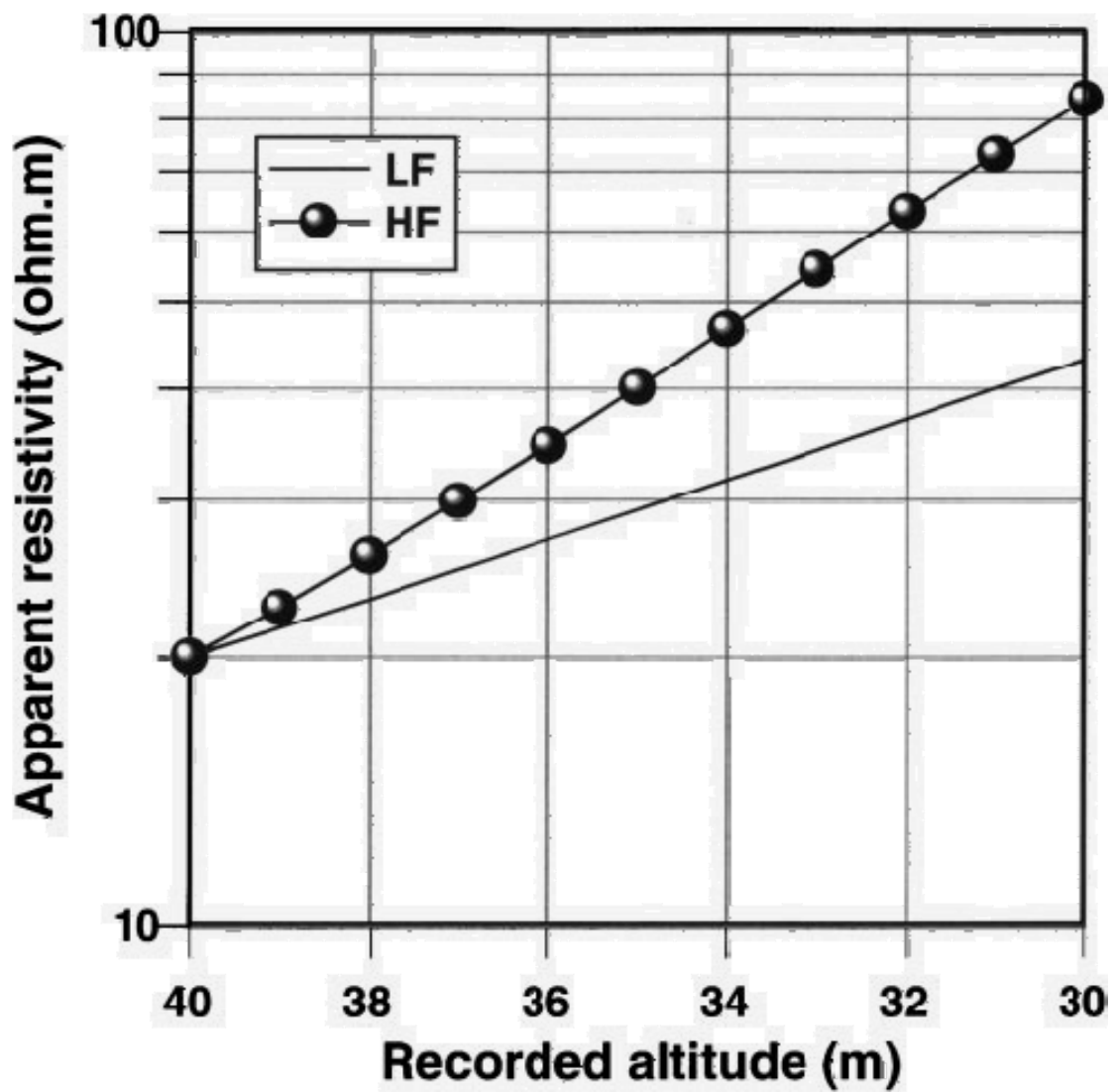


Figure 3. Apparent resistivity results obtained by numerical inversion of a $20 \Omega \text{ m}$ half-space response at 40 m. The recorded elevation is an underestimated elevation due to canopy with height ranging from 0 to 10 m. Low frequency (LF=3.1 kHz) and high frequency (HF=14.4 kHz) results

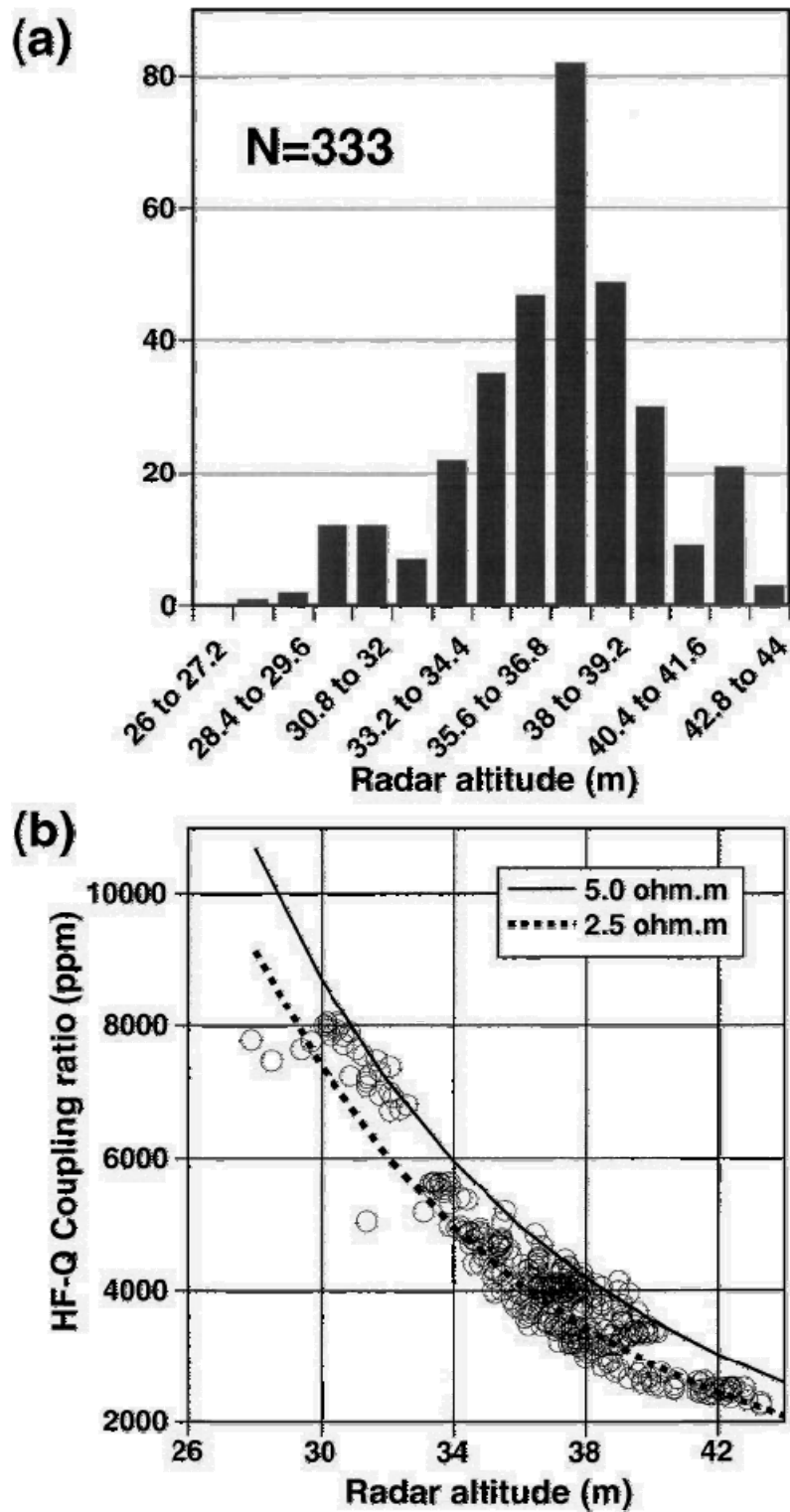


Figure 4. Survey results obtained across uniform ground (0.5×0.5 km). (a) Histogram of radar altitudes. (b) Variation of high frequency (HF=14.4 kHz), Q-component coupling ratios with radar altitude. Superimposed curves are theoretical Q-components response estimates for half-spaces of 5 and 2.5 Ω m.

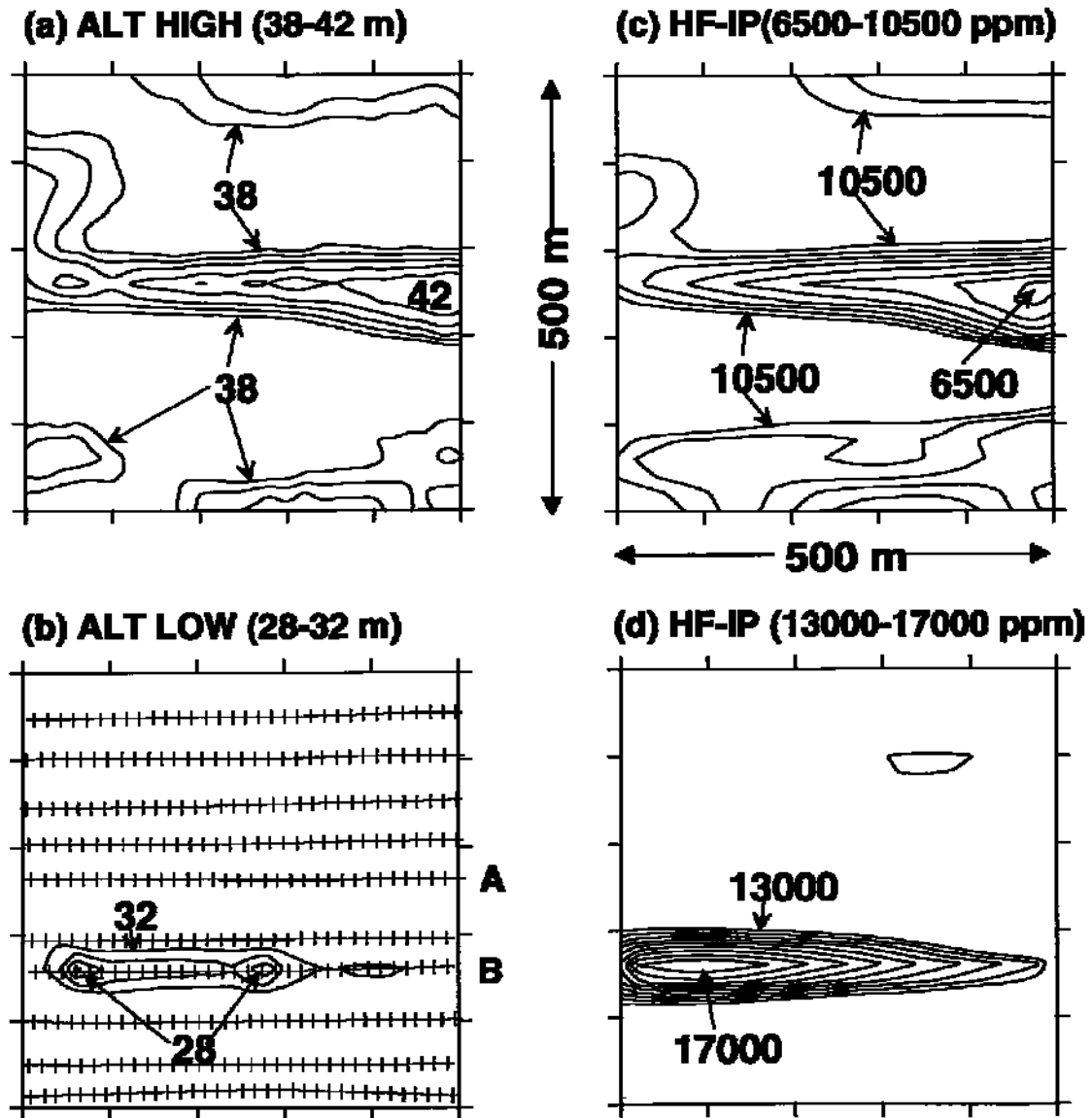


Figure 5. Survey results obtained across uniform ground (0.5×0.5 km). (a) Radar altitude in the range 38–42 m, contour interval 1 m. (b) radar altitude in the range 28–32 m, contour interval 1 m. (c) High frequency, in-phase coupling ratios in the range 6500-10500 ppm, contour interval 500 ppm. (d) High frequency, in-phase coupling ratios in the range 13000-17000 ppm, contour interval 500 ppm.

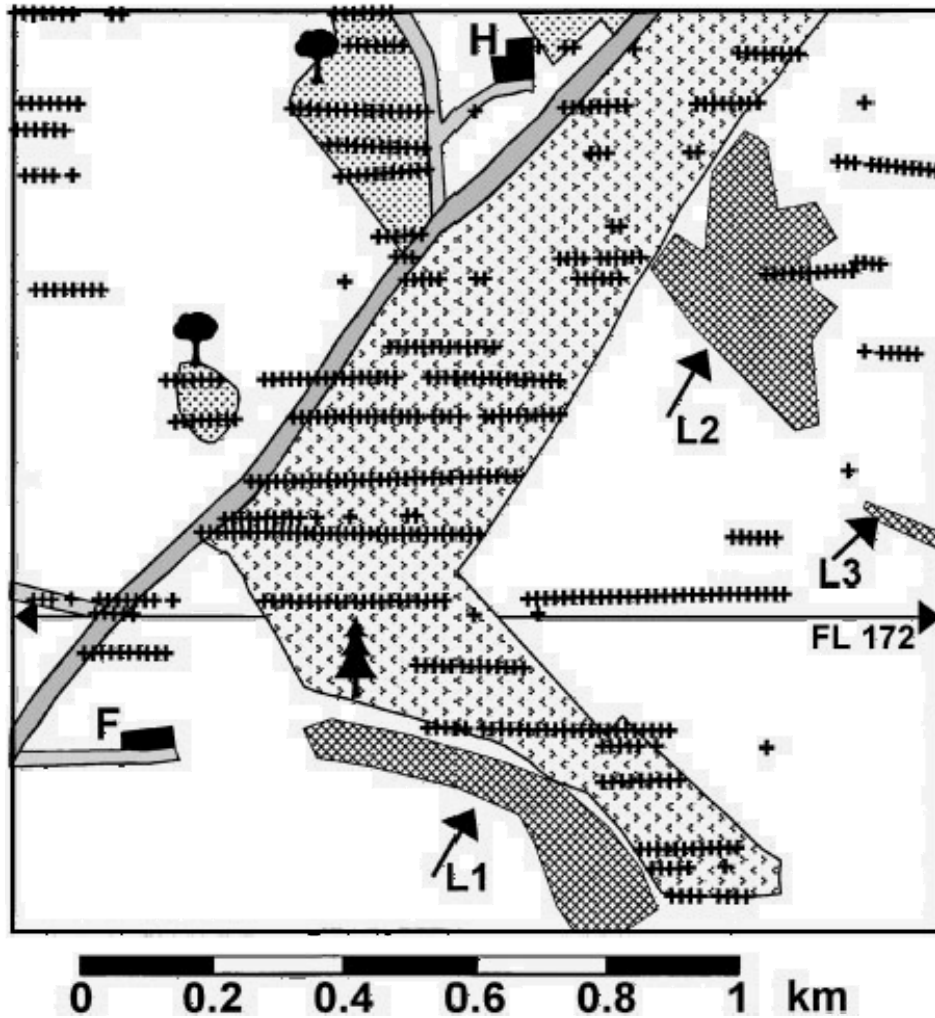


Figure 6. Map of 1.5 km × 1.5 km canopy test survey area. Canopy shown as pattern fill with symbols of tree type. F and H denote a farm and a hotel, respectively. Roads are denoted in grey. Cross symbols denote radar altitudes, along E-W flight lines, < 38 m in elevation. Three closed and covered landfills are shown as cross-hatched polygons, labeled L1, L2 and L3. Flight line (FL) 172 is shown as a horizontal line. The base map is simplified after the 1995 Ordnance Survey 1:50000 Landranger Series map.

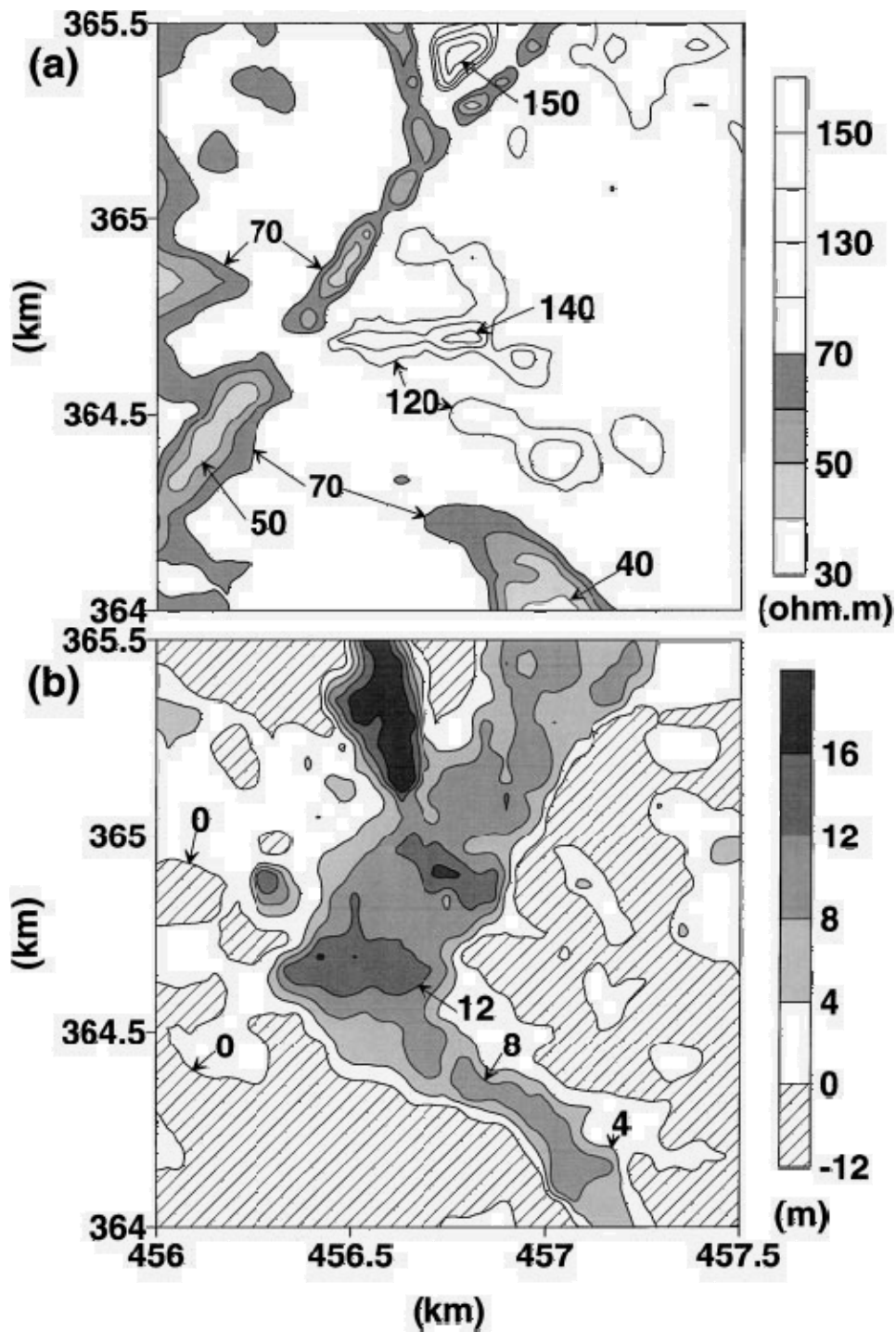


Figure 7. Conventional pseudo-layer half-space results obtained using the high frequency (14.4 kHz) data. (a) Apparent resistivity contoured as 30-70 Ω m (gray scale), 70 to 120 Ω m (line contours only). (b) Apparent depth contoured continuously, with gray scale used for values > 4 m. Negative values shown in cross-hatch

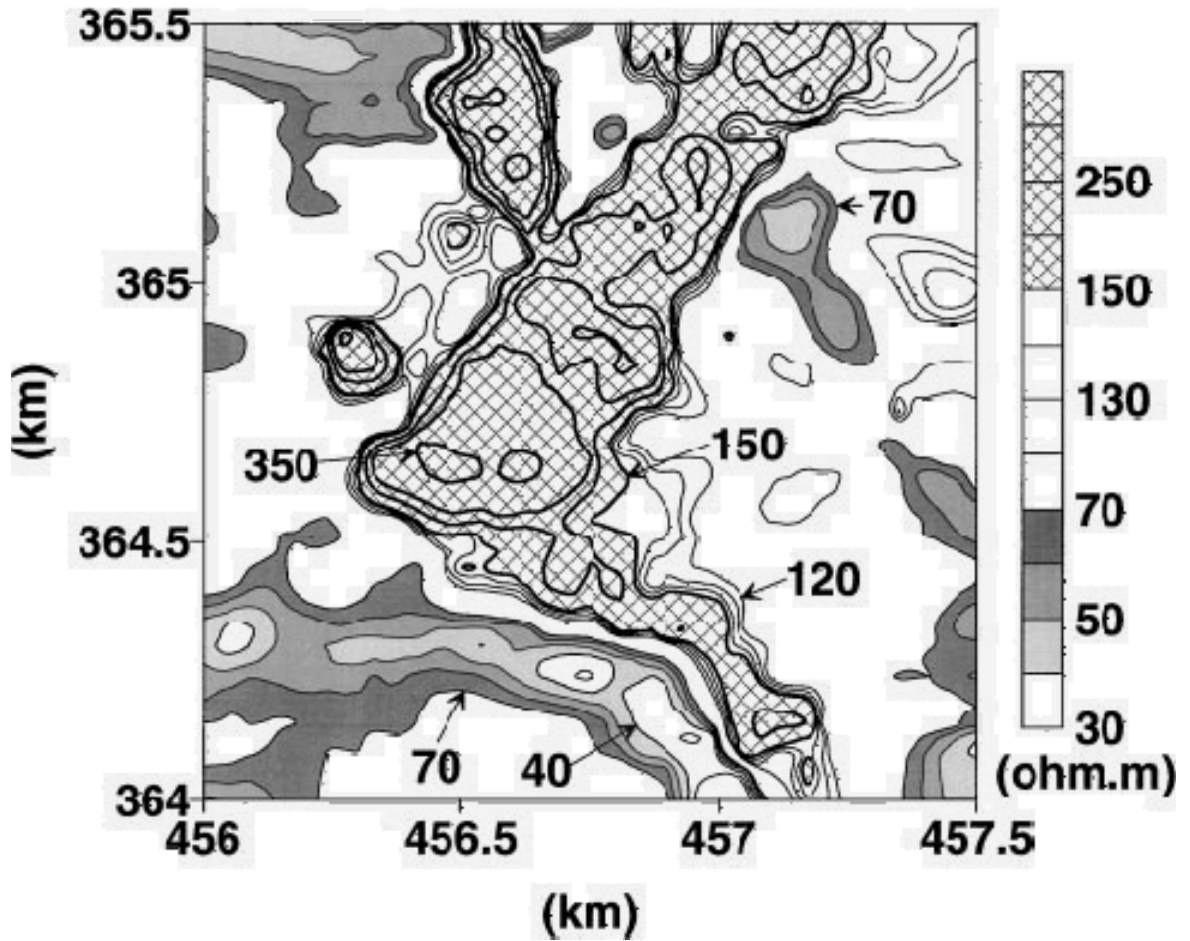


Figure 8. Half-space formal inversion results using the high frequency (14.4 kHz) data. Apparent resistivity contoured as 3-70 Ω m (gray scale), 120-150 Ω m (line only contours), 150-350 Ω m (line contours with cross-hatch).

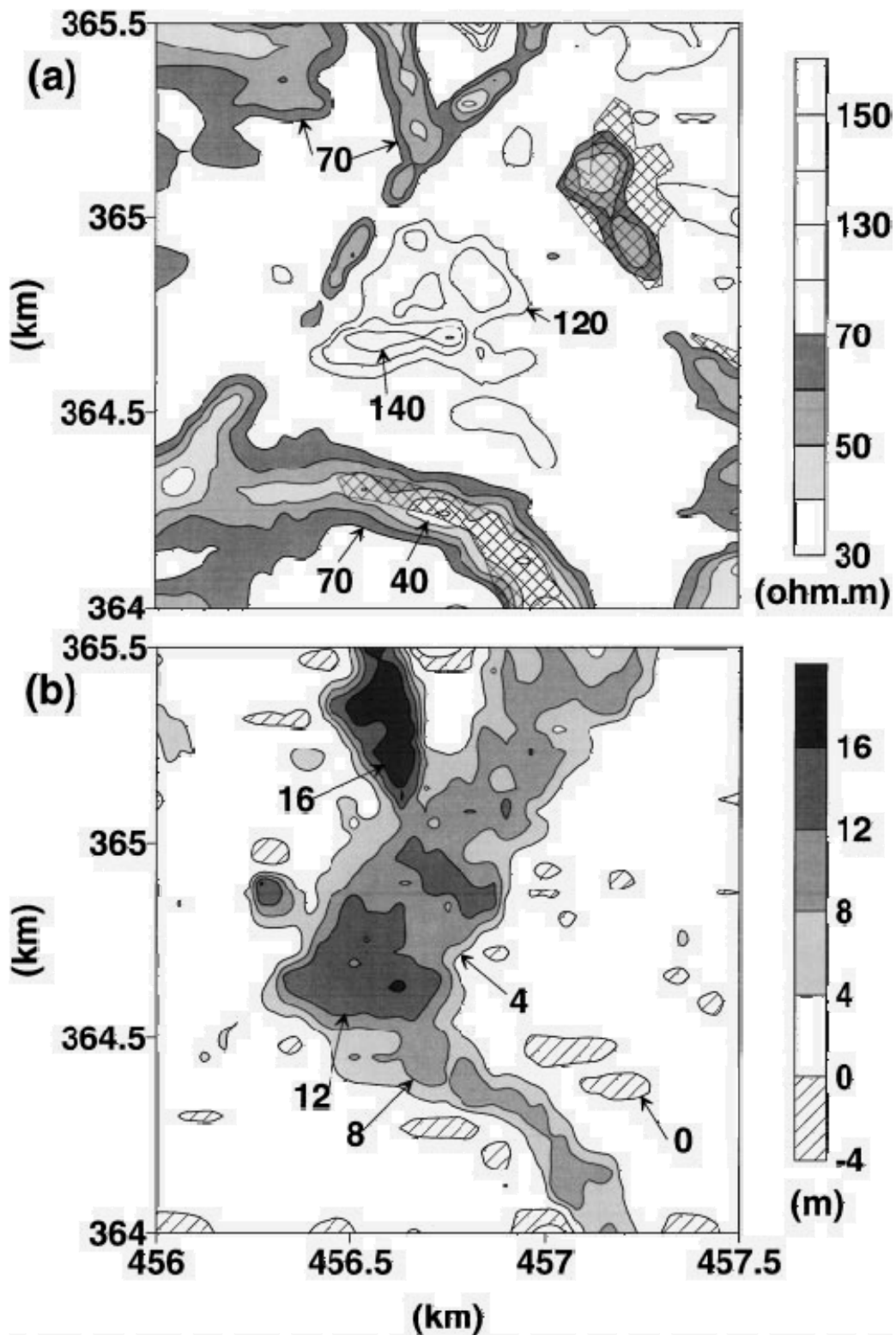


Figure 9. Formal inversion pseudo-layer half-space result obtained using the high frequency (14.4 kHz) data. (a) Apparent resistivity contoured as 30-70 Ω m (gray scale), 70 to 150 Ω m (line contours only). (b) Thickness of pseudo-layer contoured continuously, with gray scale used for values $>$ 4 m. Negative values shown in cross-hatch.

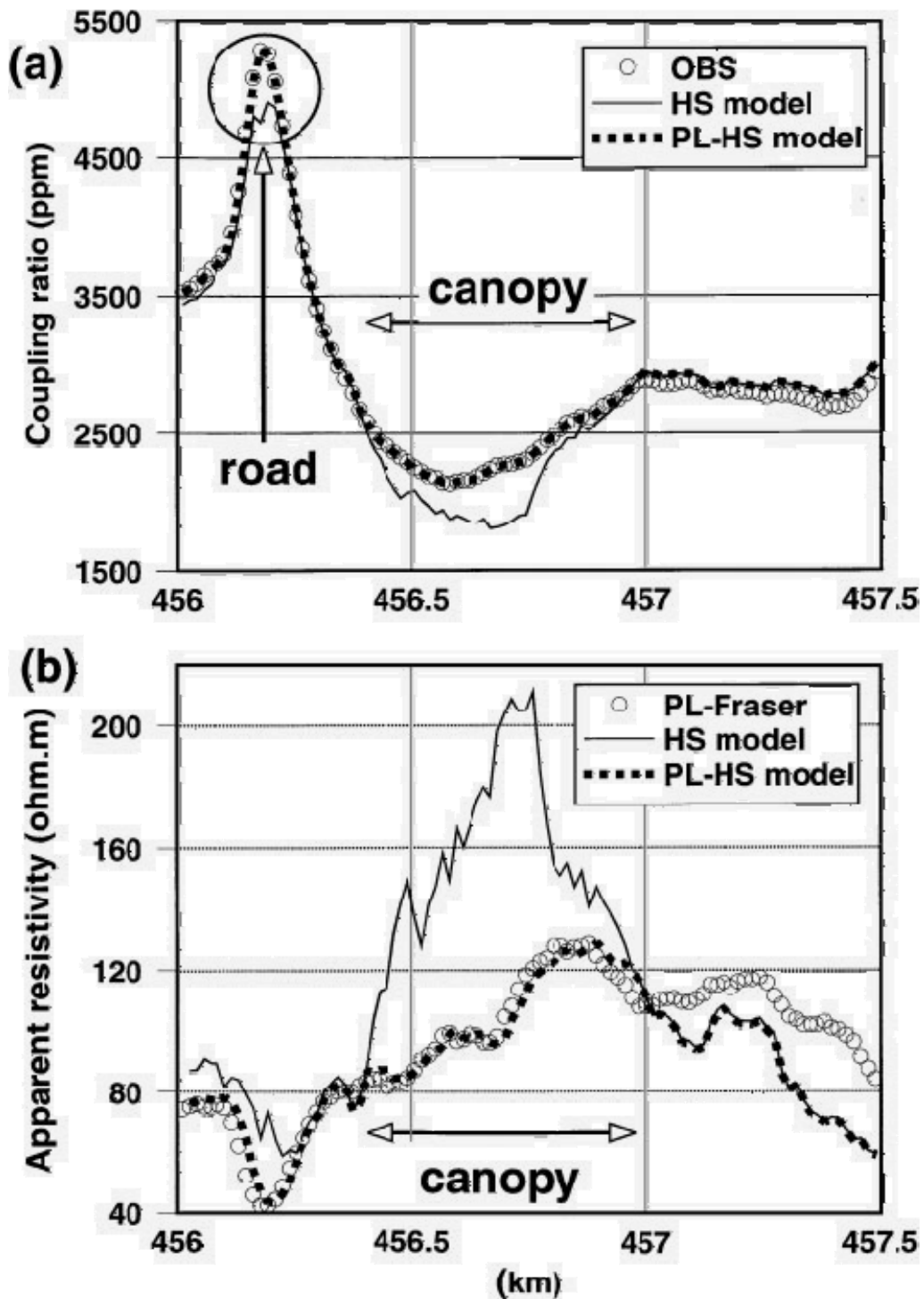


Figure 10. High frequency (14.4 kHz) observations and models obtained along flight line 172. (a) Observed IP-component (symbols), modeled IP-component response using formal half-space (HS) and pseudo-layer half-space (PL-HS) inversion. (b) Half-space apparent resistivities obtained using conventional pseudo-layer (PL-Fraser) and formal half-space (HS) and pseudo-layer half-space (PL-HS) inversion.